

# A facile LED backlight *in situ* imaging technique to investigate sub-micron level processing

Elnaz Shabani <sup>\*,1</sup>, Taslim Ur Rashid <sup>1</sup>, Russell E. Gorga, Wendy E. Krause

*Fiber and Polymer Science Program, Department of Textile Engineering, Chemistry, and Science, Wilson College of Textiles, North Carolina State University, 1020 Main Campus Drive, Raleigh, NC, 27606, USA*



## ARTICLE INFO

**Keywords:**  
LED backlighting  
Imaging  
Melt electrospinning  
Tubeless siphoning

## ABSTRACT

Many laboratory experimental techniques used for investigating fine fluid structure, such as fiber spinning, microfluidic flow, and electrospinning, require high quality images with good contrast. Common processes of observation and image recording rely heavily on highly technical light and camera setups which can be difficult to operate in some processing conditions and expensive as well. Here, we report a facile technique using LED backlight imaging to investigate ultrathin fluid profile in two different processes, melt electrospinning and tubeless siphoning. The setup comprises of a simple LED light source facing toward the camera, directly shining into the camera lens. The object under investigation was placed between the camera and the light source. The high-quality captured images and video recordings enable the precise analysis of the cone diameter and jet solidification in case of melt electrospinning, and extensional behavior profiles for tubeless siphoning. The LED backlight setup with high resolution camera is a useful tool to investigate sub-micron scale dimensions in fiber spinning, microfluidic flow, solution electrospinning, contact angle measurement for surface properties analysis, etc.

## 1. Introduction

In the manufacturing industry, *in situ* measurement is a widespread need for inspecting processing conditions. Many processes need high spatial resolution (from micron to sub-micron) imaging techniques that are viable to localize for *in situ* imaging. Examples of scientific applications that require such photography are electrospinning, contact angle measurement for surface properties analysis, fiber spinning, extensional viscosity measurement, etc. For example, in melt electrospinning, it is crucial to investigate micron scale dimensions to precisely analyze the jet stability, cone diameter and jet solidification zone, and correlate them to the process parameters such as electric field intensity, plate to collector distance or temperature for optimizing the process. Tubeless siphoning, which is a useful tool to explore extensional flow profile of non-Newtonian fluids, also needs clear visualization of thin siphon line, especially in case of low viscosity fluids. To date, various imaging techniques have been developed and utilized for analyzing industrial processing both qualitatively and quantitatively [1–6]. The most common inspection method uses a camera to acquire two dimensional images of the system under investigation [7]. Matthys reported a flow

visualization technique to investigate extensional flow profile for tubeless siphoning of polymeric fluids by using intense ultraviolet (UV) light generated by a pulsed nitrogen laser [3]. The technique was based on the activation of a photochromic dye by illuminating from the side with a very short pulse of UV light focused in a small beam at the location of interest. The photoactivation resulted in the apparition of dark marker lines in the center of the siphoned fluid which allowed to record high speed movies to compute velocities anywhere inside the flow field. Later on, another group of researchers used NMR microscopy to observe the velocity profiles directly at any point of the tubeless siphon column of viscoelastic fluid (polyethylene oxide (PEO) in water) [2]. The technique was efficient to measure the radial profiles of axial velocity in the siphon flow; however, it was comparatively expensive and not convenient for industrial implementation. While investigating electrospinning jet stabilities for PEO-water, Shin et al. used area backlight to improve the contrast of the images that were taken on conventional film using high-speed photographic techniques [8]. The technique used multiple equipment arrangement that might not be feasible to perform *in situ* measurements. Thoppey et al. used a halogen lamp and/or a light source comprised of a square array of white LEDs to illuminate polymer jets to

\* Corresponding author.

E-mail address: [eshabani@ncsu.edu](mailto:eshabani@ncsu.edu) (E. Shabani).

<sup>1</sup> The Authors contributed equally.

record images of the electrospinning process of PEO solutions for further analysis [9]. They tinted the polymer solution with a dye to provide enhanced imaging contrast for viewing the jet initiation process and subsequent stabilized jets.

Most of the imaging techniques used by the researchers are either complicated in design or not cost effective. Some setups use dye molecules for improved visualization of the process, which are difficult to implement in large scale industrial setting. Moreover, current methodologies often require a microscope that even though very precise, is not flexible enough to be properly localized for a specific application especially in cases where *in-situ* photography is needed. In addition, the direct use of light source from the same side of the camera suffers from non-uniform illumination caused by the light source and the surrounding environment. To overcome these problems, in recent years, researchers emphasize using backlight technique for imaging objects or in-line processing [7,10–13]. In backlight setup, the object is placed between the camera and the light source that enables shining the camera lens directly. Chen et al. presented smartphone supported backlight illumination technique for microfluidic imaging [11]. However, the complicated imaging box system restricts their design from ubiquitous applications. In a recent work, Liu et al. also utilized backlight technique using an incandescent lamp for optical observations of droplet-jet shape to guide adjustments to optimize and maintain fiber diameter in online controlled electrospinning of PEO solution [13]. However, they used a microscopic lens attached with a single-lens reflex camera to observe and record the process that might not be convenient for universal use and cost effective as well. In a recent study, Wunner et al. used two cameras to capture the flight path and fiber diameter on the collector in a melt electrowriting process [14]. In this technique the first camera was placed at a distance of 100 mm to focus on the region of the fiber flight path and the second camera was a microscopic camera with 10× magnification lens. The images from this technique appear as a dark line in front of an illuminated background with no detailed information of the inside jet. The images were utilized for high throughput analysis of the melt electrowriting process parameters to develop the best processing conditions among the many parameters affecting the jet diameter. The necessity for small distance of the camera to the object and the utilization of the microscopic camera could potentially complexify the setup design in large scale applications.

In this paper we introduce a simple yet versatile photography technique that can be utilized to take *in situ* still images from sub-micron scale objects with high resolution that enables post-processes measurements and analysis. Our study aims to develop a simple but accurate tool to acquire both qualitative and quantitative information about the subject. We use a LED lamp as a source of light and a digital single-lens reflex camera (DSLR) or a smartphone for capturing image or video. The capability of this technique is investigated for various areas of research including 1) melt electrospinning, and 2) tubeless siphoning, showing the broad ranges of applicability. For melt electrospinning, images are collected for further analysis on the jet cone size, jet number and jet diameter at the initiation, and the solidification point of the jet during the process. For tubeless siphoning, applicability of the technique to collect high quality images and videos for measuring extensional behavior of the fluids is investigated. We demonstrate that this simple imaging setup is applicable to a variety of laboratory and industrial processing.

## 2. Methodology

### 2.1. Backlight setup

The backlighting setup comprises of a light source, namely a LED lamp that is placed in such a way as to directly shine the camera lens. The object is placed between the camera and the light source. The purpose is to signify the edges of the object in the illustration which will ultimately enable us to perform precise dimension analysis for the

specific application. (Fig. 1). We used a simple LED lamp (33 LED Super Bright Wardrobe Lights, Portable Magnetic Stick Wireless, geometry 9.5 inch by 1.5 inch by 0.7 inch, manufacturer: CHNXU). This LED lamp minimizes the environment lighting compared to the translucent lamp used by Liu et al. [13]; hence, the focused light coming from the LED source shines the camera lens effectively. Both a high-quality Canon DSLR (Canon EOS Rebel T5i with 18–135 mm EF-S IS STM Lens, single flexible zoom lens, 18.0 Megapixel CMOS sensor, able to take both color and black and white images, pixel pitch: 4.29  $\mu\text{m}$ , pixel area: 18.40  $\mu\text{m}^2$ , and pixel density: 5.43 MP/cm<sup>2</sup>) and simple smartphone (Samsung Galaxy J7 Prime; 13 MP Sony Exmor RS, f/1.9 aperture, zoom levels: 4x) cameras have been utilized in this work to show the versatility of this technique with ranges of camera specifications. However, in the case of sub-micron scale dimensions, high resolution cameras will get more precise images.

In the case of the Canon DSLR camera, the settings need to be manually adjusted properly for backlit photography. The three main setting parameters that need to be adjusted are as following: aperture, shutter speed, and ISO (International Organization for Standardization) speed. Aperture is the opening in a lens through which light passes to enter the camera. A larger aperture allows more light to enter the camera. The shutter speed determines how long shutter remains open as the picture is taken. The slower the shutter speed, the longer the exposure time. The shutter speed and aperture together control the total amount of light reaching the sensor. However, for backlit photography, especially in the cases where the object is favored to be isolated from the background, adjusting the aperture to a wider degree (means lower number e.g. f/5.6) and adjusting the light based on the shutter speed is recommended. As the light source is positioned behind the object and is directly lighting the lens, a higher shutter speed, (e.g. 1/1000) is recommended to minimize the exposure of the camera to the light. The third important parameter to be adjusted is the ISO speed which determines the sensitivity of the camera sensors to the light and for this technique is recommended to be adjusted to the lower degrees. The settings that were adopted in this work were: ISO speed: 200, f1/5.6 and shutter speed 1/1000. The camera setting for Samsung Galaxy J7 Prime is much straightforward. We used automatic mode of the camera with occasional adjustment of the zoom (up to 4x) with manual focusing.

### 2.2. Melt electrospinning setup

A free surface melt electrospinning setup was utilized to fabricate micron scale fibers of linear low density polyethylene (LLDPE) (granule, ASPUN 6850 Fiber Grade Resin with the melt index of 30 g/min under 190 °C/2.16 kg based on the data sheet provided by the manufacturer; Supplier: Dow Chemical company) [15]. The apparatus consists of an aluminum sharp edge plate and a commercial hot plate (Fisher Scientific, model: HP88857100) to heat up the source plate. The source plate is a hand-made aluminum plate with the surface area of 13.6 × 4.8 cm and edge walls of 1 mm thickness and 0.8 cm height on the sides (with no wall on the sharp edge where fibers are formed). The source plate

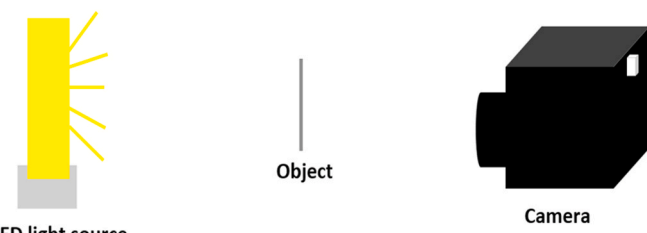


**Fig. 1.** Schematic configuration of a backlighting setup. The object is placed in between the camera and the LED light source. The distance between the LED and the object is 10–20 cm, and that between the object and the camera is 10–50 cm.

temperature is set to 190 °C. One side of the source plate is connected to a k-type thermocouple to monitor the temperature of the source plate. The opposite side of the plate is attached to ground wire. The counter electrode consists of a square aluminum plate with the surface area of 30 × 30 cm that is connected to the negative polarity of a high voltage source (Glassman, Model FC60R2). The entire apparatus is placed in a wood chamber with transparent acrylic plastic as front door and top wall to observe the process. The thermocouple reader is placed outside the box, however for the schematic purposes it is shown inside the chamber. [Fig. 2](#) illustrates the schematic design of the melt electrospinning setup.

### 2.3. Tubeless siphoning setup

Some non-Newtonian fluids, such as polymer solutions with sufficient entanglements or polymer melts have a special ability to form a tubeless siphon (ductless siphon). [Fig. 3](#) depicts a set up for tubeless siphoning of 2% (w/w) solution of polyethylene oxide (PEO) (MW 400,000; supplier: Scientific Polymer Products, INC.) in water. When the glass pipette nozzle (connected to a tube and vacuum source) is inserted into the PEO solution, a siphon starts first. The siphoning action continues when the nozzle is raised above the free surface of the fluid. The non-Newtonian viscoelastic stresses, resulting from stretching of the polymer molecules in solution, support the weight of the jet against the gravitational force [16]. This technique has been used to investigate the extensional properties of the non-Newtonian fluids [3,17]. Here, an LED backlighting technique is utilized (as illustrated in [Fig. 3](#)) for the close investigation of the extensional behavior of PEO solution by measuring siphon height and change in siphon diameter with respect to axial distance from the solution surface.

## 3. Results and discussion

### 3.1. Melt electrospinning

Decreasing fiber diameter has been a long-lasting and challenging goal of the researchers in the melt electrospinning process due to the high viscosity nature of the polymer melt. Attempts have been taken to reduce the melt viscosity including temperature change and incorporation of additives or plasticizers that have been effective in reducing the fiber diameter [18]. Using conductive additives have also been reported to be effective in reducing the fiber diameter due to an increase in the melt conductivity [19,20]. However, no systematic method was utilized to capture the jet behavior to fundamentally study the mechanisms of the modification in each of the cases. An *in situ* observation of the jet formation in the electrospinning process enabled us to precisely measure

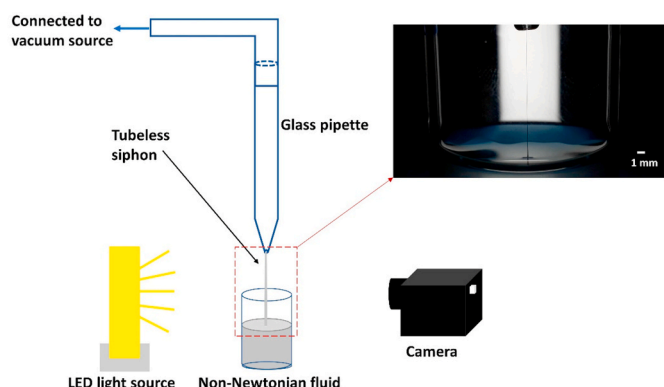


**Fig. 3.** Schematic of the tubeless siphoning PEO solution with backlight photography setup. The fluid reservoir is placed in between the LED light source and camera for better visualization of the thin siphon line. The distance between the LED and the object is 15 cm, and that between the object and the camera is 10 cm. Images are taken during siphoning operation and are used to investigate siphon line profile. The image of the tubeless siphoning used here is for 2% (w/w) PEO solution (in water), taken by smartphone camera (Samsung Galaxy J7 Prime).

the formed cones diameter and correlate that to the modification mechanisms that are being employed ultimately to further optimize the process. More importantly, *in situ* observation in electrospinning entails inherent limitations due to the high voltage utilization that inhibits close shots. Utilizing a backlight sharpens the edges of the objects, facilitating the size or shape analysis from the taken images even in lower resolutions taken from long distances ([Fig. 4-a](#)).

### 3.1.1. Cone diameter analysis

Fabrication of sub-micron fibers have long been desired for many applications including filtration, tissue engineering, drug delivery, etc. There are many factors in an electrospinning process that control the final fiber diameter. In a free surface electrospinning, precise control of the cone diameter at the initiation is crucially important. Factors including voltage, distance, or temperature can have a huge effect on the cone diameter. Having a systematic design to take *in situ* picture of the cones enable us to control the final fiber diameter. Utilizing the backlit setup in [Fig. 2](#), an *in situ* picture was taken from a single cone during the process ([Fig. 4-a](#)). Using ImageJ software, the diameter of the cone at the initiation point as well as the diameter of the jet immediately after formation is measured. This is a useful information especially in a free surface electrospinning where no nozzle or spinneret is utilized to

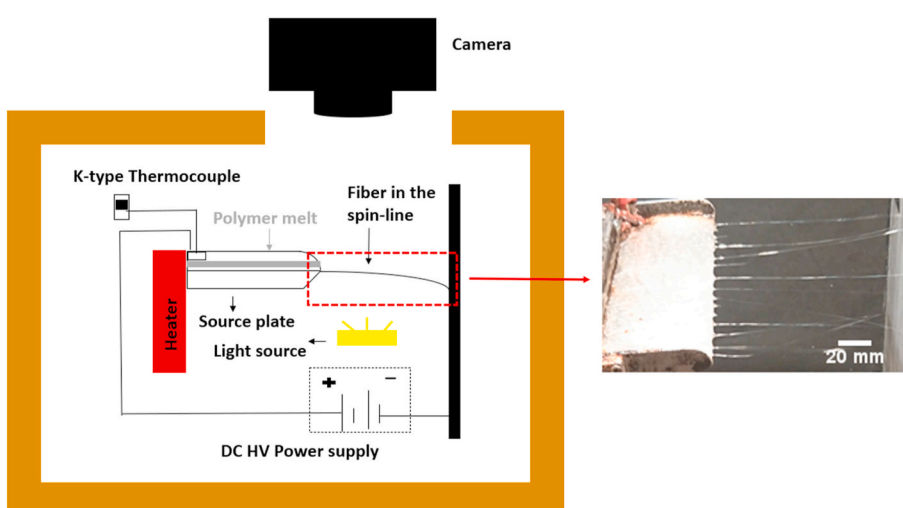


**Fig. 2.** Schematic of the melt electrospinning apparatus for PE with backlit photography setup; the light source is placed behind the spinning jets, directly shining the camera lens. The distance between the LED and the object is 18 cm, and that between the object and the camera is 43 cm. With utilizing this technique *in situ* still images were taken from the process as well as the jets for further analysis on the cone size, jet number, jet diameter at the initiation and the solidification point of the jet as it goes through a phase change during the process. The image is added to illustrate the overview of the spinning location and is taken via a side-lit setup and the phone camera. The side-lit setting illuminates the entire plate and give a better overview of the entire process where the aim is not on the detailed analysis of the jet.

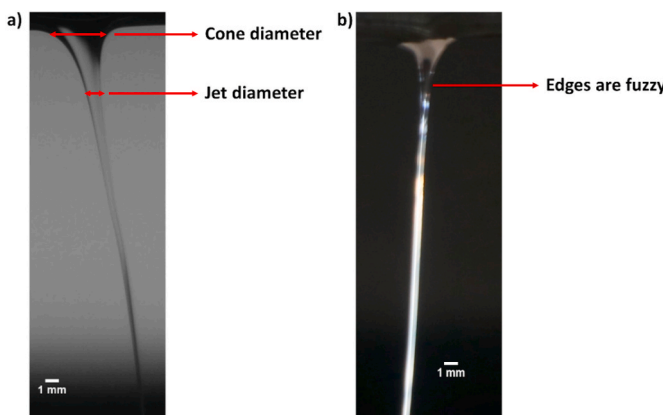


**Fig. 4.** Picture of a single jet taken *in situ* in the melt electrospinning process of PE utilizing a) backlit setup b) side-lighting setup. The backlit image of the jet provides clear edges for precise measurements while the side lighting image shows fuzzy edges with over illumination. The experiment conditions were: distance from the plate to collector 10 cm, voltage 40 kV, in an open environment temperature. The cone diameter obtained was  $2.9 \pm 0.9$  mm (at the initiation of the process) and  $1 \pm 0.1$  mm (after 20 min run of the process).

control the formation of the cones. For comparison, a picture was taken utilizing a side-lighting setup. In side-lighting the light source was placed on one side of the setup, shinning the jets from the side angle. As observed in Fig. 4-b, this method of lighting does not offer enough clarity and the edges of the object tend to be fuzzy and over illuminated.

### 3.1.2. Jet solidification

In many fiber processing techniques, fibers are fabricated through a jet formation followed by a phase change, usually solidification, process. In fiber melt processing, the solidification of the jet happens through heat transfer with the surrounding environment. After the solidification, no more stretching can be applied to the jet that could affect its properties including diameter. Monitoring the solidification point throughout the jet *in situ* is very important. So far, there is no effective visual technique to be utilized to observe the phase change in a fiber spinning process. In a solidification process, a transparent liquid phase transforms into an opaque solid phase. This transparency transformation creates a significant light contrast which can be captured by utilizing a backlit setup (Fig. 5). As observed in Fig. 4-b, side-lighting does not provide this visual of the jet. The solidification point here is reported to occur within 0.7 cm of the length of the jet. Such a short solidification distance was previously identified by Zhmayev et al. and referred to electrohydrodynamic jet quenching in melt electrospinning process [21]. Knowing the solidification information would enable researchers to have a precise control over the solidification point by controlling the parameters affecting the phase change, (e.g. spin-line temperature, and the subsequent heat transfer process in the case of melt electrospinning) that significantly affects the final fiber morphology and properties.

### 3.2. Tubeless siphoning

Extensional viscosities for non-Newtonian fluid can be estimated by the tubeless siphon technique where the liquid is continuously drawn into a capillary with raising the tube above the liquid surface forming a column, as shown in Fig. 6 [22,23]. Having a stress-free boundary, tubeless siphoning is often considered to be wholly extensional, which is one of the major prerequisites for extensional viscosity measurement technique. The maximum height of siphon ( $h$ ) is used to characterize the ratio  $(\eta_E/\eta)$  of non-Newtonian fluids, where  $\eta$  is shear viscosity, and  $\eta_E$  is extensional viscosity. An approximate hydrodynamic analysis shows  $\eta_E/\eta \sim (h)^2$  [17]. However, clear visualization of siphon line is challenging to measure, especially in case of low viscosity polymer solutions.

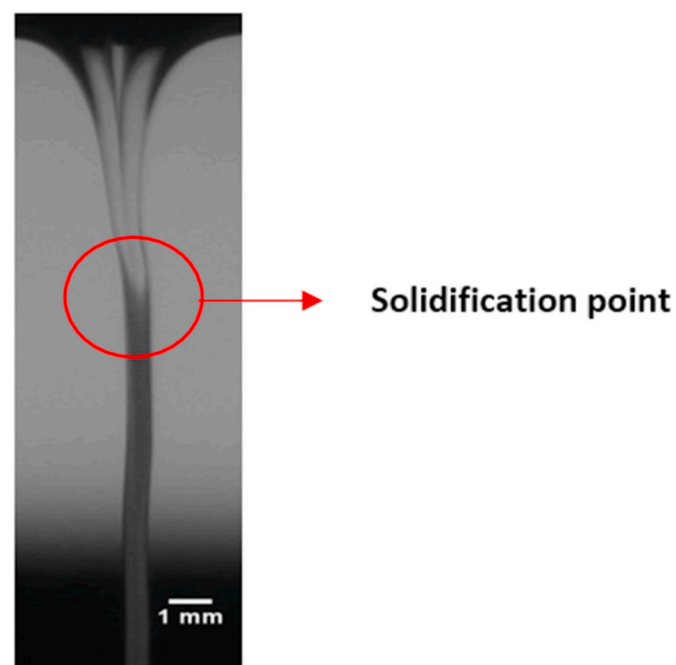


**Fig. 5.** Visualization of the *in-situ* solidification of the jet in the melt electrospinning process utilizing backlight setup. The side-lit image does not capture the solidification point.

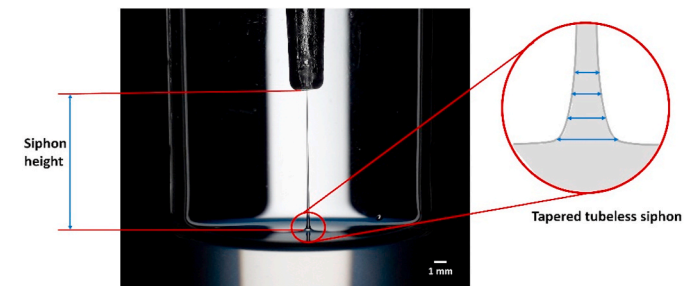


**Fig. 6.** Illustration of siphon height and diameter measurement from images with improved contrast. The inset shows the gradual change in siphon diameter with axial distance from liquid surface for an extremely thin siphon line. Siphon diameter at different heights can be measured to investigate extensional behavior of different polymer solutions. The image of the tubeless siphoning used in the figure is for 2% (w/w) PEO solution (in water).

Fig. 6 illustrates how siphon height can be measured from high resolution images taken from a video. The maximum siphon height can be calculated from the images by using ImageJ software. This measurement can successfully replace the manual measurement of the height by using measuring scale.

Moreover, as seen in Fig. 6, the column diameter decreases with distance from the fluid surface to the pipette entrance. This gradual decrease in diameter is needed to balance gravitational stress by increasing mean velocity component along the column [2]. A correlation between siphon height and diameter can be established to investigate extensional behavior of different polymer solutions. Images taken at different magnifications under backlight setting will be a potential tool to analyze the profile of extremely thin siphon lines which are not visible at certain height with the naked eye.

## 4. Conclusion

We have demonstrated a facile technique to acquire visual information using a simple LED backlight setup. The use of this imaging

technique may allow to precisely analyze the processing profiles of melt electrospinning and tubeless siphoning of polymer fluids. A detailed quantitative analysis of these effects will be presented in future publications. The report presented herein could potentially be extended to in-line real-time determination of the sub-micron scale dimensions in fiber spinning, microfluidic flow, solution electrospinning, contact angle measurement for surface properties analysis, etc., where the output could be used to adjust the feeders.

#### CRediT authorship contribution statement

**Elnaz Shabani:** Conceptualization, Data curation, Formal analysis, Funding acquisition, Investigation, Methodology, Software, Supervision, Validation, Visualization, Writing - original draft, Writing - review & editing. **Taslim Ur Rashid:** Conceptualization, Data curation, Formal analysis, Investigation, Methodology, Software, Validation, Visualization, Writing - original draft, Writing - review & editing. **Russell E. Gorga:** Funding acquisition, Project administration, Resources, Supervision, Writing - review & editing. **Wendy E. Krause:** Project administration, Resources, Supervision, Writing - original draft, Writing - review & editing.

#### Declaration of competing interest

The authors declare that they have no known competing financial interests or personal relationships that could have appeared to influence the work reported in this paper.

#### Acknowledgement

This work was partially funded by the National Science Foundation (CMMI #1635113).

#### References

- [1] Y. Murai, K. Inaba, Y. Takeda, F. Yamamoto, Backlight imaging tomography for slug flows in straight and helical tubes, *Flow Meas. Instrum.* 18 (5–6) (2007) 223–229.
- [2] Y. Xia, P. Callaghan, Imaging the velocity profiles in tubeless siphon flow by NMR microscopy, *J. Magn. Reson.* 164 (2) (2003) 365–368.
- [3] E.F. Matthey, Measurement of velocity for polymeric fluids by a photochromic flow visualization technique: the tubeless siphon, *J. Rheol.* 32 (8) (1988) 773–788.
- [4] K.S. Bronk, K.L. Michael, P. Pantano, D.R. Walt, Combined imaging and chemical sensing using a single optical imaging fiber, *Anal. Chem.* 67 (17) (1995) 2750–2757.
- [5] D. Glick, P. Thiansathaporn, R. Superfine, In situ imaging of polymer melt spreading with a high-temperature atomic force microscope, *Appl. Phys. Lett.* 71 (24) (1997) 3513–3515.
- [6] J.C. De Anda, X. Wang, X. Lai, K. Roberts, K. Jennings, M. Wilkinson, D. Watson, D. Roberts, Real-time product morphology monitoring in crystallization using imaging technique, *AIChE J.* 51 (5) (2005) 1406–1414.
- [7] B.L. Quist, Method and Apparatus for Backlighting and Imaging Multiple Views of Isolated Features of an Object, Google Patents, 2006...
- [8] Y. Shin, M. Hohman, M. Brenner, G. Rutledge, Experimental characterization of electrospinning: the electrically forced jet and instabilities, *Polymer* 42 (25) (2001), 09955-09967.
- [9] N.M. Thoppey, J. Bochinski, L. Clarke, R.E. Gorga, Edge electrospinning for high throughput production of quality nanofibers, *Nanotechnology* 22 (34) (2011) 345301.
- [10] Y. Murai, H. Oiwa, T. Sasaki, K. Kondou, S. Yoshikawa, F. Yamamoto, Backlight imaging tomography for gas–liquid two-phase flow in a helically coiled tube, *Meas. Sci. Technol.* 16 (7) (2005) 1459.
- [11] G. Chen, H.H. Chai, L. Yu, C. Fang, Smartphone supported backlight illumination and image acquisition for microfluidic-based point-of-care testing, *Biomed. Opt. Express* 9 (10) (2018) 4604–4612.
- [12] U. Kanade, B. Ganapathy, Camera Placed behind a Display with a Transparent Backlight, Google Patents, 2011..
- [13] S. Liu, D.H. Reneker, Droplet-jet shape parameters predict electrospun polymer nanofiber diameter, *Polymer* 168 (2019) 155–158.
- [14] F.M. Wunner, P. Miesczanek, O. Bas, S. Eggert, J. Maartens, P.D. Dalton, E.M. De-Juan-Pardo, D.W. Hutmacher, Printomics: the high-throughput analysis of printing parameters applied to melt electrowriting, *Biofabrication* 11 (2) (2019), 025004.
- [15] Q. Wang, C.K. Curtis, N.M. Thoppey, J.R. Bochinski, R.E. Gorga, L.I. Clarke, Unconfined, melt edge electrospinning from multiple, spontaneous, self-organized polymer jets, *Mater. Res. Express* 1 (4) (2014), 045304.
- [16] R.B. Bird, R.C. Armstrong, O. Hassager, *Dynamics of Polymeric Liquids*, 1, Fluid mechanics, 1987.
- [17] K.K. Chao, M.C. Williams, The ductless siphon: a useful test for evaluating dilute polymer solution elongational behavior. Consistency with molecular theory and parameters, *J. Rheol.* 27 (5) (1983) 451–474.
- [18] T.M. Robinson, D.W. Hutmacher, P.D. Dalton, The next frontier in melt electrospinning: taming the jet, *Adv. Funct. Mater.* 29 (44) (2019) 1904664.
- [19] S. Malakhov, S. Belousov, A. Bakirov, S. Chvalun, Electrospinning of non-woven materials from the melt of polyamide-6 with added magnesium, calcium, and zinc stearates, *Fibre Chem.* 47 (1) (2015) 14–19.
- [20] E. Shabani, C. Li, R. Komer, L. Clarke, J. Bochinski, R. Gorga, B. Boland, N. Sheoran, Strategies to improve the unconfined melt electrospinning process via incorporation of ionically conductive particles, *Bull. Am. Phys. Soc.* 64 (2019).
- [21] E. Zhmayer, D. Cho, Y. Lak Joo, Electrohydrodynamic quenching in polymer melt electrospinning, *Phys. Fluid.* 23 (7) (2011), 073102.
- [22] S. Peng, R. Landel, Preliminary investigation of elongational flow of dilute polymer solutions, *J. Appl. Phys.* 47 (10) (1976) 4255–4260.
- [23] R. Balmor, Steady and unsteady isochoric simple extensional flows, *J. Non-Newtonian Fluid Mech.* 2 (4) (1977) 307–322.